Traction motor optimization using mesh reshaping for gradient evaluation

---

Article:

Gerber, S., Wang, R-J. (2020) Traction motor optimization using mesh reshaping for gradient evaluation, *Proc. of XXIV International Conference on Electrical Machines*, (ICEM), pp. 2546--2552, 23-26 August 2020, Gothenburg, Sweden (virtual conference)

ISBN: 978-1-7281-9944-3 / IEEE Catalogue Number: CFP2090B-USB

Traction Motor Optimization Using Mesh Reshaping for Gradient Evaluation

Stiaan Gerber and Rong-Jie Wang

***Abstract*—Optimization of electrical machines is a challenging task that can be solved using either gradient based or non-gradient based methods. While gradient based methods are theoretically much more efficient, their performance is often compromised in applications where finite element analyses are used for performance evaluation. In this paper, a common pitfall of gradient evaluation and a method for overcoming it is discussed. A special gradient based optimization approach that employs mesh reshaping for gradient analyses and standard remeshing for other steps is proposed. The performance of this optimization approach is evaluated in a representative case study of a traction motor design optimization. The results clearly highlight the benefits of the mesh reshaping technique.**

***Index Terms*—Design optimization, finite element analysis, gradient methods, mesh refinement, permanent magnet motors, traction motors**

I. Introduction

ELECTRICAL traction motors are widely employed in various types of drive systems. With the increasing level of electrification of transport systems, the amount of traction motors being deployed will surely see significant growth. Considering this trend, the design optimization of traction motors is vitally important as ever more stringent constraints are placed on the performance and cost of these motors.

Traction motor optimization is generally a more difficult task in comparison with the optimization of motors designed for a single operating point. These motors have to satisfy different constraints in various operating points, including start-up, base speed and maximum speed. Furthermore, overload and partial load conditions at various speeds may impose yet more constraints on the design. Considering that the number of variables that describe the geometry of traction motors typically fall in the range of 10 - 20, the optimization task may be challenging.

Several different optimization strategies may be formulated, with differences in terms of the selection of variables, operating points and analysis procedure [1]. Despite these differences, a distinction can generally be made between gradient based methods and non-gradient based (global) methods.

The intricate cross-sectional geometries of traction motors necessitate the use of numerical methods for accurate solution of the magnetic fields and subsequent performance analysis. In this regard, the finite element method is ubiquitous. However, due to the computational cost of finite element analyses, it is important that optimization strategies that rely on finite element analyses to evaluate the objective function and constraints be efficient. In many scenarios, the use of global optimization algorithms is not very practical because of the computational cost of an analysis and the large number of analyses required to find an optimal design. Gradient based algorithms generally require far fewer function evaluations to converge and therefore, they may be a better choice for many problems, especially those where the objective and constraints are relatively smooth functions. This includes many problems in traction motor optimization.

Even though gradient based algorithms are theoretically more efficient than global methods, in practice, gradient based optimization using finite element analyses does not always live up to its potential. One issue, that is the focus of this paper, is the accuracy and stability of the gradient calculations. Gradients have to be estimated numerically by perturbation of the design variables. When small changes are made to the geometry, the structure of the resulting finite element mesh may change significantly. The change in the structure of the mesh has an impact on the calculated gradient.

It has been recognized that changing the structure of the mesh can be detrimental to the performance of optimization procedures, either for issues related to accuracy or simply because generating new meshes takes a significant amount of time [2]–[7]. In [2], a method is proposed whereby the structure of the mesh can be maintained while accommodating changes in the geometry with as little displacement of nodes as possible. It was proposed that optimization can be performed without changing the structure of the mesh at all using this technique. Other mesh deformation techniques have also been proposed and applied to 3-D problems, where the cost of mesh generation can be especially high [5]–[7].

In this paper, a unique implementation of a gradient based optimization procedure for traction motors will be described and evaluated. In this implementation, meshes used for gradient evaluation are generated using the technique proposed in [2] (reshaping), but meshes for other function evaluations are generated anew (remeshing). In this way, the accuracy of gradients and the quality of meshes is maintained over large search spaces, allowing powerful and flexible optimization procedures to be developed. Unlike some other works that make use of mesh deformation [4]–[7], the primary goal

This work was supported in part by the National Research Foundation of South Africa and ABB Corporate Research, Sweden.

S. Gerber and R-J. Wang are with the Department of Electrical and Electronic Engineering, Stellenbosch University, Stellenbosch, 7600, South Africa (e-mail: sgerber@sun.ac.za, rwang@sun.ac.za)

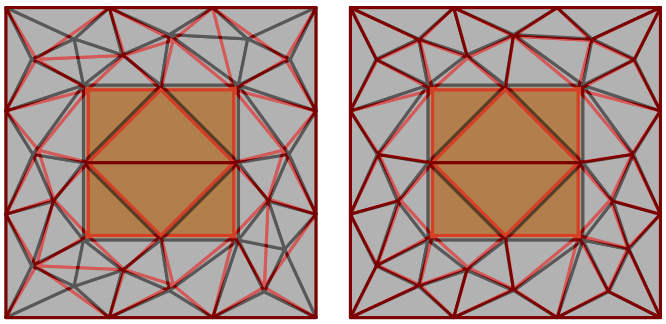

(a) Remeshing (b) Reshaping

Fig. 1. Remeshing vs reshaping of a base mesh. Base mesh in black, modified mesh in red.

is not to avoid or reduce the cost of mesh generation, but the improvement of the performance of the optimization algorithm, for which accurate gradient information is vital.

II. Meshing Procedure

In this section, an overview of the special meshing procedure used during gradient evaluation is given. In this paper, the method is referred to as mesh *reshaping*. The method was first proposed in [2], where it is described in some detail. Here, practical issues regarding the specific implementation used in this work is discussed.

The method allows the structure of a mesh to be maintained while accommodating small variations in the geometry. As an example, Fig. 1 shows a simple square mesh with an inner square feature. Fig. 1a illustrates what can happen when the size of the inner square is reduced and the mesh is regenerated anew (standard remeshing). The original mesh is shown in black and the modified mesh in red. Notice that the structure of the modified mesh (red) is different from the base mesh (black) since some elements have "flipped". On the other hand, Fig. 1b illustrates a modified mesh generated using the reshaping method. The structure of the mesh is maintained and nodes have been displaced a minimum amount to accommodate the change in size of the inner square.

The reshaping procedure can be considered to consist of three steps: node classification, constrained node displacement calculation and free node displacement calculation.

A. Node classification

In the first step, all nodes of the base mesh have to be classified as either free nodes or constrained (fixed displacement) nodes. All nodes that are directly related to the geometry are constrained nodes. These nodes typically lie on the boundaries of uniform regions. The best way to identify these nodes will depend on the underlying mesh generator. In this study, the input to the mesh generator is a planar straight-line graph (PSLG), as shown in Fig. 2. The constrained nodes can be identified by finding all the nodes in the base mesh that lie on an input segment of the PSLG. The number of constrained nodes may exceed the number of nodes in the PSLG since some input segments may be subdivided by the mesher.

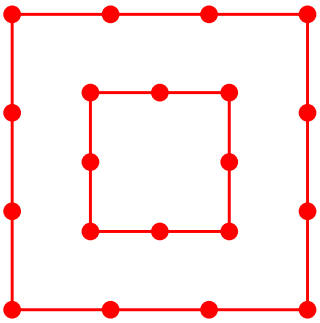

Fig. 2. Planar straight-line graph from which constrained nodes are identified.

B. Constrained node displacement calculation

Having identified the free and constrained nodes in the base mesh, the next step is to determine the displacement of the constrained nodes in the modified mesh. This is achieved by comparing the PSLG of the base mesh to the PSLG of the desired modified mesh. It is important to ensure that the structures of the two PSLGs match precisely for this technique to work effectively. If this is ensured, it is straightforward to calculate the displacement between matching nodes. The displacement of constrained nodes in the mesh that do not appear in the PSLGs (those that have been generated by subdivision of input segments) are determined by interpolation of the displacements of the nodes that do appear in the PSLGs.

C. Free node displacement calculation

In the final step, the displacements of all the free nodes, $\mathbf{d_f}$, are solved using Laplace's equation [2], subject to the boundary conditions on the constrained nodes, $\mathbf{d_i}$:

$$\nabla^2 \mathbf{d} = 0 \tag{1}$$

$$\mathbf{d_i} = \mathbf{p_i^{mod}} - \mathbf{p_i^{base}} \tag{2}$$

$$\mathbf{d} = \mathbf{d_f} \cup \mathbf{d_i} \tag{3}$$

where

$$\mathbf{d} = \begin{bmatrix} d_x \\ d_y \end{bmatrix} \quad \text{and} \quad \mathbf{p_i} = \begin{bmatrix} x \\ y \end{bmatrix} \tag{4}$$

are vectors of displacements and nodal positions, respectively.

While it is noted in [2] that the above procedure described in this section may fail for large displacements of the input nodes, this is not a concern when using the procedure in the proposed optimization strategy. Since mesh reshaping is only applied for gradient evaluation and the displacement of the input nodes is always small when the design variables are perturbed by small values, the mesh reshaping procedure works reliably without any additional stabilization procedures. Furthermore, remeshing ensures that the quality of

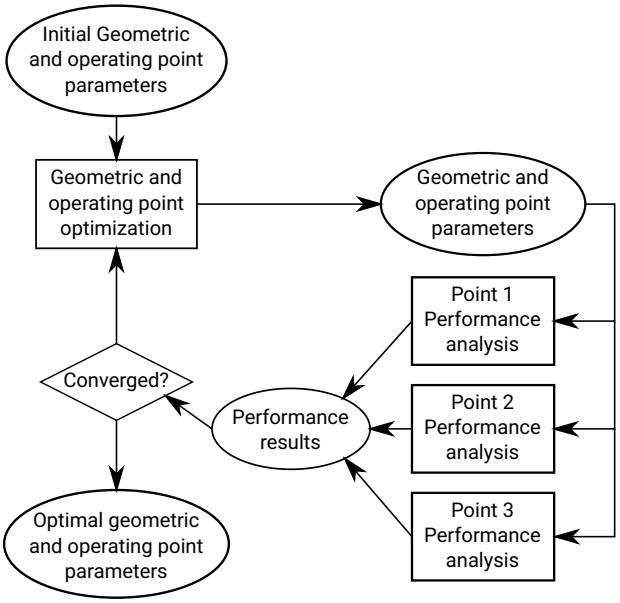

Fig. 3. Flow diagram of the optimization process where geometric and operating point variables are optimized together in a single loop.

the mesh is maintained over a large design space. Using a single base mesh and reshaping for an entire optimization process may lead to poor quality meshes being generated during optimization.

III. Optimization Strategy

A gradient-based optimization strategy is considered where the aforementioned mesh reshaping strategy is applied during gradient evaluation. In this work, the SLSQP algorithm [8] available in the Python SciPy package is used.

A. Problem formulation

For traction applications, it is important to consider the performance of the machine in several operating points [9], [10]. One approach to traction motor design is to conduct a full drive cycle analysis for each candidate design. For this type of analysis, flux maps are typically generated from which the machine's performance can be evaluated in many operating points with relatively low computational cost. Using the flux maps, optimal dq-currents can be found for each required torque-speed operating point. However, generating the flux map is a computationally expensive process.

In this work, an alternative approach is used, as depicted in Fig. 3. Instead of conducting a complete drive cycle analysis, the focus falls on a number of critical operating points. If a relatively low number of points can be considered, this strategy is efficient compared to approaches that require flux maps. The considered operating points may include peak overload conditions at low and high speed and continuous operating points where the machine will operate for a large percentage of time. Alternatively, the points may be spread across the entire operating region, according to the specific requirements of the application. For each considered operating point, a set of constraints is introduced in the optimization problem to ensure satisfactory performance. Typically, these constraints include the required torque and limits on the voltage, current and losses. Other aspects such as demagnetization may also be considered for each operating point.

TABLE I
Costs of materials

Material	Cost
Permanent magnet	\$50/kg
Lamination steel	\$2/kg
Copper	\$6.67/kg

B. Design variables

As shown in Fig. 3, the optimization process consists of a single loop where geometric and operating point variables are optimized alongside each other. The operating point variables consist of the dq-currents for each operating point. Thus, if three operating points are considered, as in Fig. 3, a total of six operating point variables are added to the set of design variables.

During optimization, each design geometry is not necessarily evaluated at its optimal operating point. However, a successful optimization will ensure that both the geometry and the operating variables converge to optimal values for each operating point.

IV. Traction Motor Case Study

In this section, a case study is presented to evaluate the performance of optimization using standard remeshing and the reshaping technique for gradient evaluation. An interior permanent magnet (PM) machine with a V-shaped magnet configuration is designed with the objective of minimizing the active material cost. The active material cost was calculated based on the values given in Table I.

A. Design variable selection

The motor topology considered in this case study is shown in Fig. 4. The major geometric parameters that describe the topology are illustrated in Figs. 5a and 5b. Some transformations are applied to these parameters to obtain the geometric design variables defined in the optimization problem. This is done in order to ensure that the search space can be bounded properly and that all points within the search space yield valid geometries. The most important design variables are described here, with some simplifications to keep the discussion brief.

For this case study, the outer diameter $2(R_o)$ was fixed at 250 mm. The stator inner radius, R_i, was obtained from the ratio of the stator thickness to the total machine thickness, $\frac{R_o - R_i}{R_o - r_i}$. This ratio was chosen as a design variable. The inner rotor radius, r_i, was chosen as a design variable. The expression, $\frac{H_s}{H_s + H_y}$, was chosen as a design variable, from

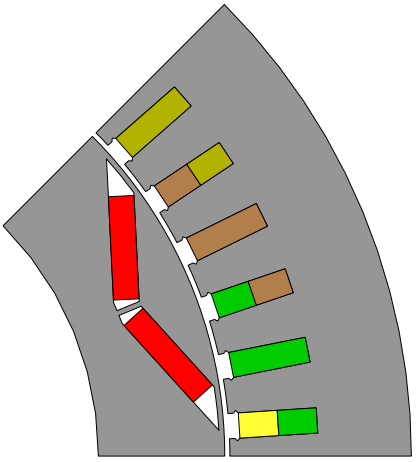

Fig. 4. Interior PM topology considered in the case study.

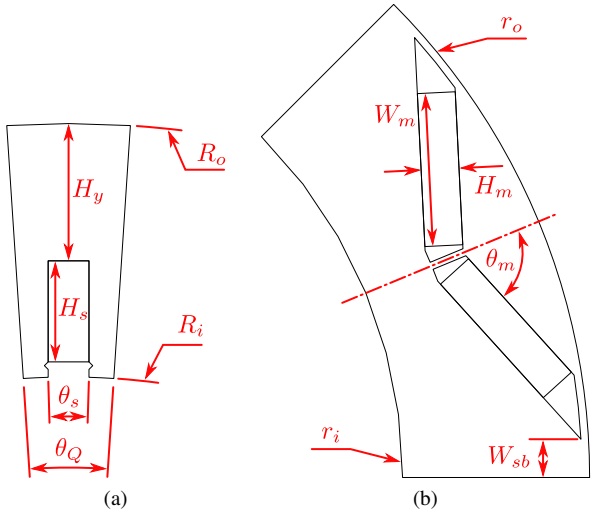

Fig. 5. Geometric parameters. a) Stator parameters. b) Rotor parameters.

which H_s and H_y was calculated. The stator slot width was obtained from the ratio $\frac{\theta_s}{\theta_Q}$. This ratio was also chosen as a design variable.

For the rotor, the width of the gap between flux barriers, W_{sb}, was chosen as a design variable. The angle of the magnets, θ_m, was chosen as a design variable, although in practice, this variable was normalized relative the minimum and maximum feasible angles for a specific rotor size. Another parameter related to the aspect ratio of the magnets, $\frac{W_m}{H_m}$, was used as a design variable. The thickness of all connecting bridges were fixed.

In addition, the stack length and the number of series turns were chosen as design variables.

B. Specifications

The specifications for the motor are given in Table II. As can be seen in the Table, three operating points have been chosen to consider in the optimization. The position of these operating points within the torque-speed envelope of the machine is shown in Fig. 6. Notice also that there is a large difference in the acceptable loss between the overload operating points and the continuous operating point.

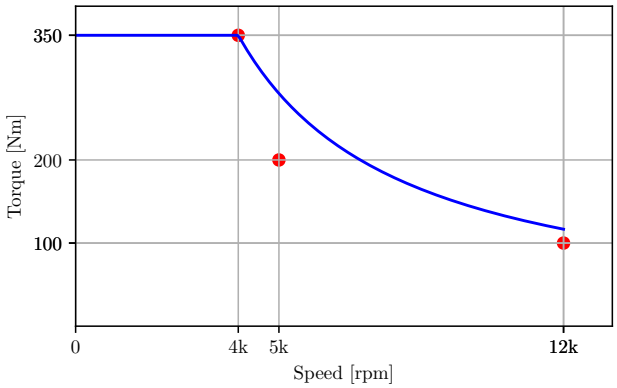

Fig. 6. Location of operating points considered in optimization within the torque-speed envelope of the machine.

TABLE II
TRACTION MOTOR SPECIFICATIONS

Geometry	
Number of poles	8
Number of slots	48
Outer diameter	250 mm
Air-gap length	1 mm
Material characteristics	
Winding fill factor	0.65
PM remanent flux density	1.184 T
PM recoil permeability	1.052
Lamination steel	M400-50A
Inverter output limits	
Line voltage	230 V
Phase current	500 A
Point 0: Peak overload (Low speed)	
Torque	350 Nm
Speed	4000 rpm
Loss	10 kW
Point 1: Continuous (Base speed)	
Torque	200 Nm
Speed	5000 rpm
Loss	4.2 kW
Point 2: Peak overload (Max speed)	
Torque	100 Nm
Speed	12 000 rpm
Loss	10 kW

C. Optimization

A set of 80 random initial designs were generated within the design space. Starting from each of these initial design points, the machine was optimized using the two different meshing strategies for gradient evaluation: remeshing and reshaping. The objective was to minimize the active material cost. Four constraints were applied to each operating point, corresponding to limits on the torque, voltage, current and the loss. The loss calculation only included DC conduction

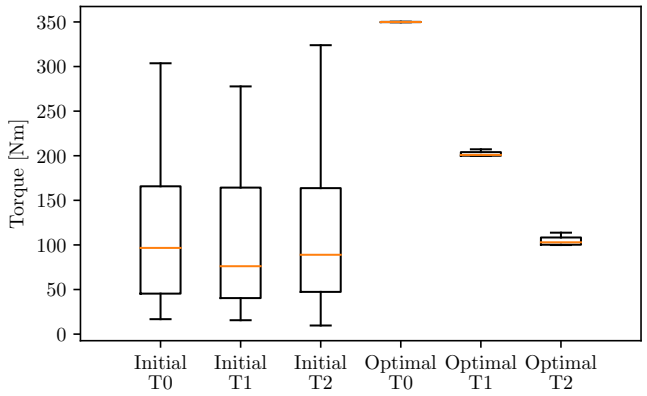

Fig. 7. Initial and optimal design torque distributions for each operating point.

loss and core loss. This was done to reduce computational costs for the purpose of this paper, but of course other loss components could also be included in the analysis.

Thus, a total of 160 optimization problems were solved. The optimizations were run on an Intel i7-3770K CPU @ 3.5 GHz and completed in approximately 15 hours. Relatively coarse meshes were employed to limit the computational time. The average mesh size was roughly 1000 elements.

D. Results

Figs. 7 - 10 show the distributions of the torque, voltage, current and loss for each operating point for both initial designs and optimum designs. In these figures, the distributions are shown using box plots. The whiskers (lower and upper horizontal lines) show the 5th and 95th percentiles of the data, while the lower and upper edges of the box correspond to the first and third quartiles of the data. The horizontal line inside the box represents the median of the data.

The data shown in these figures include the results from both optimization strategies. As expected, the initial values of the constrained functions are distributed over a wide range and in many cases the constraints are violated. On the other hand, the values of the constrained functions at the optimum design points are tightly grouped at the constraint boundaries. This is indicative of successful optimizations. In Fig. 11, it can also be seen that the distribution of the cost is more tightly grouped for the optimum designs compared to the initial designs, although not as tightly grouped as the constraints are. This indicates that all the optimizations did not quite manage to find the best optimum point.

The performance of the remeshing and reshaping optimization strategies are compared in Figs. 12 and 13. In Fig. 12, it can be seen that optimization using reshaping managed to converge to an optimal solution using a significantly lower amount of function evaluations on average compared to the standard remeshing approach. Furthermore, Fig. 13 shows that optimization using reshaping managed to find better optimum designs with lower cost.

In order to better understand why optimization using reshaping showed improved performance, the advantage of

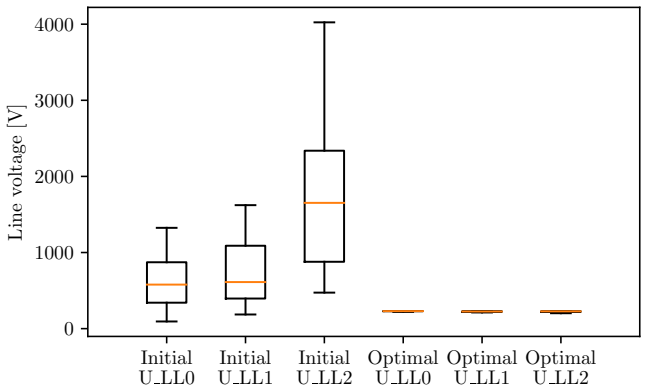

Fig. 8. Initial and optimal design line voltage distributions for each operating point.

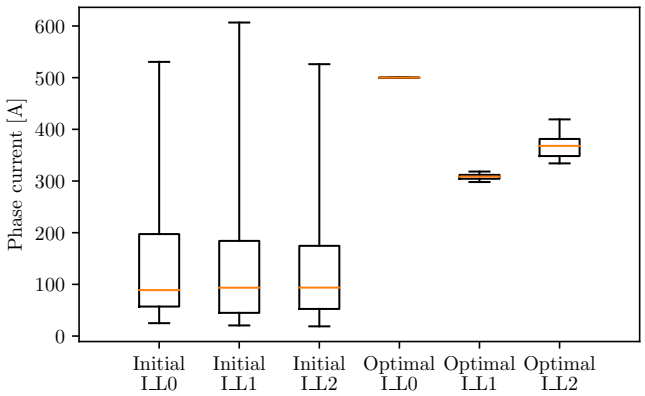

Fig. 9. Initial and optimal design phase current distributions for each operating point.

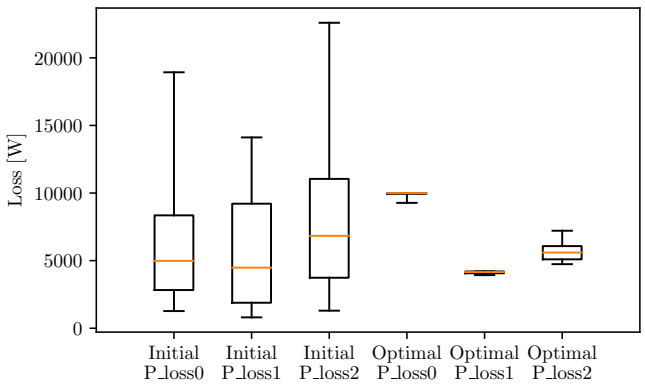

Fig. 10. Initial and optimal design loss distributions for each operating point.

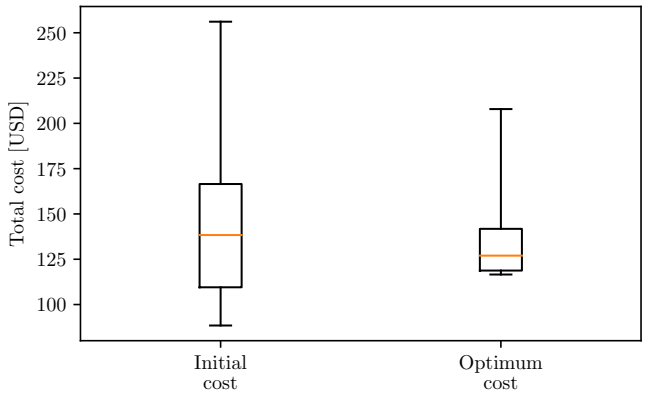

Fig. 11. Initial and optimal design cost distribution.

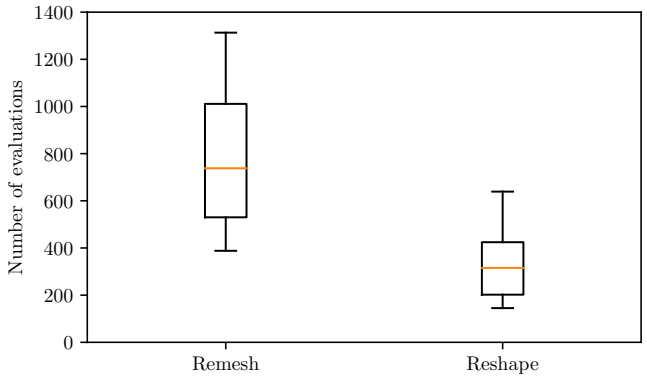

Fig. 12. Total number of function evaluations per optimization for remeshing and reshaping optimization strategies.

the reshaping technique for gradient calculation is investigated further. Figs. 14 and 15 illustrate the gradient of the maximum overload torque with respect to a subset of the design variables, calculated at the best optimum design point. The gradient is calculated as the change in the torque divided by the change in the design variable for different relative step sizes. A zero gradient means that the overload torque is independent of a specific variable. In Fig. 14, it can be seen that the gradient varies significantly as the

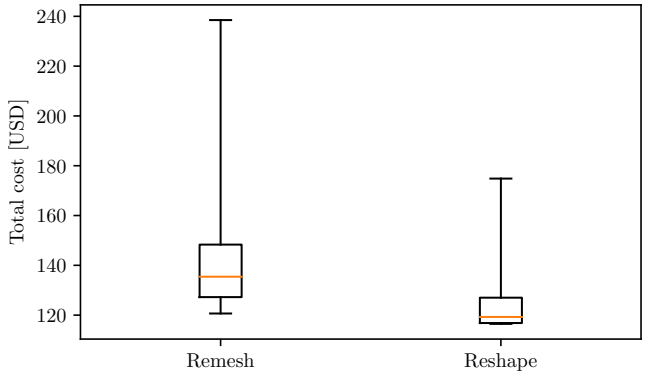

Fig. 13. Objective function (total cost) at the optimum for remeshing and reshaping optimization strategies.

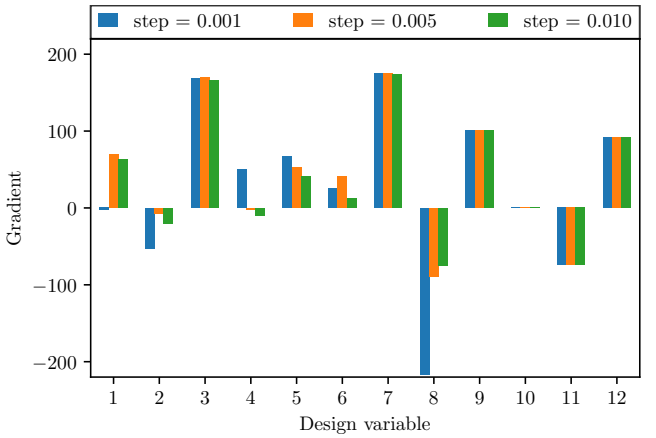

Fig. 14. Gradient of the maximum overload torque with respect to the design variables, calculated using standard remeshing.

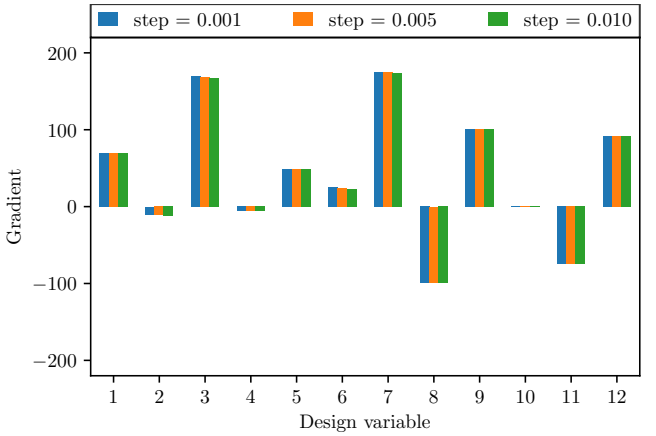

Fig. 15. Gradient of the maximum overload torque with respect to the design variables, calculated using mesh reshaping technique.

step size is changed, even changing sign in some cases. In Fig. 15, the situation is greatly improved as the gradient is virtually independent of the step size. This illustrates the improved stability of the gradient calculation using the reshaping technique and is the reason for the improvement in the performance of the optimizations that use reshaping.

The smoothness of the objective function and two constraints are further evaluated in Fig. 16 along a specific search direction, corresponding to the gradient of the objective function. The two considered constraints are the line voltage in point 1 and the torque in point 2. The solid lines were obtained using remeshing while the dotted lines were generated by reshaping, using the point with a step size of zero as a base mesh. Again, it is clear that the remeshing strategy produces a significant amount of noise in the output for fine step sizes, while the reshaping strategy eliminates these errors. On the other hand, discrepancies between the results from the remeshing and reshaping strategies for larger steps sizes, as observed in Fig. 16a around a step size of 0.5, are likely due to a degradation in the quality of the reshaped mesh. This illustrates why it still better to employ remeshing for larger step sizes.

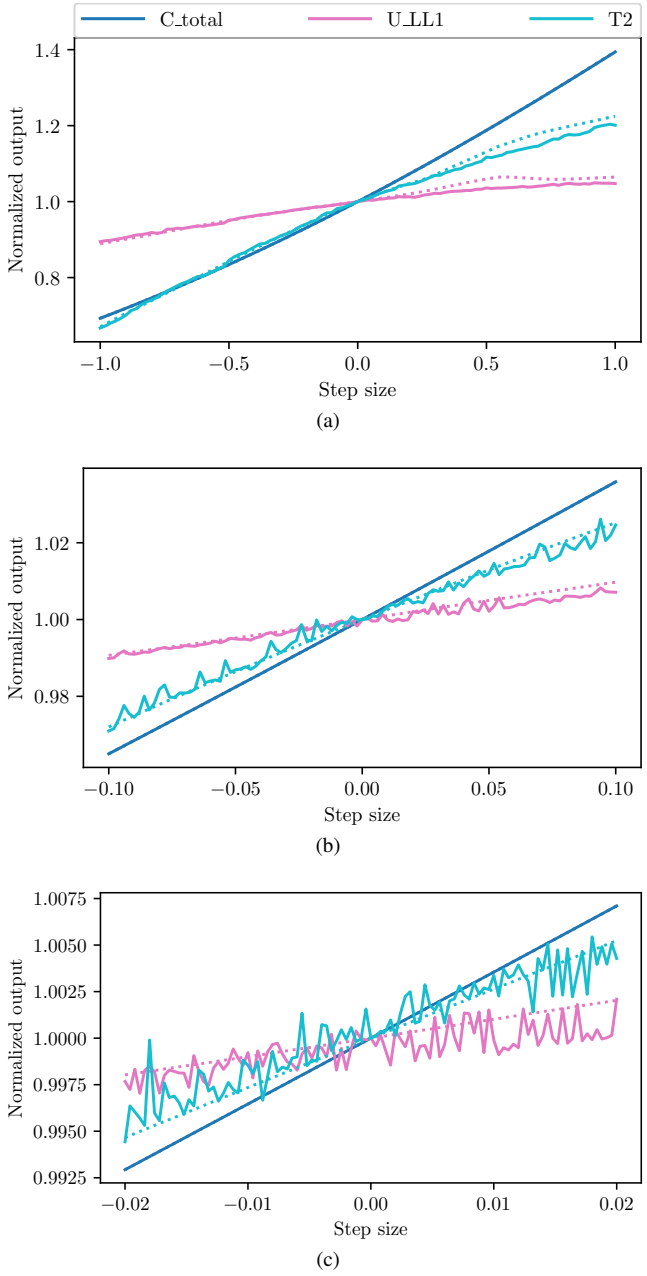

Fig. 16. Evaluation of the objective (C_total) and two constraints (U_LL1 and T2) in the direction of the gradient of the objective.
Solid lines: Remeshing. Dotted lines: Reshaping.

V. Conclusion

Gradient evaluation is a common pitfall in the application of gradient based optimization to traction motor design. In this paper, it has been demonstrated that a special mesh reshaping technique can lead to significant improvements in the performance of gradient based optimization when applied in the calculation of gradients. Standard remeshing can still be used in other steps of the optimization algorithm. In this way, the stability of the gradient calculation is improved while mesh quality is maintained over a large design space.

Mesh reshaping techniques are not commonly available in commercial electromagnetic finite element simulation packages. This paper makes a strong case for the inclusion of such techniques.

While the focus of this paper falls on the electromagnetic design of traction motors, the technique is just as applicable to many other disciplines where gradient based optimization using finite element analyses can be employed. Similar performance gains may be expected. The technique may also be extended to 3-D optimization processes.

References

[1] G. Bramerdorfer, J. A. Tapia, J. J. Pyrhnen, and A. Cavagnino, "Modern Electrical Machine Design Optimization: Techniques, Trends, and Best Practices," *IEEE Trans. Ind. Electron.*, vol. 65, no. 10, pp. 7672–7684, Oct. 2018.

[2] K. Yamazaki, H. Ishigami, and A. Abe, "An Adaptive Finite Element Method for Minor Shape Modification in Optimization Algorithms," *IEEE Trans. Magn.*, vol. 44, no. 6, pp. 1202–1205, Jun. 2008.

[3] S. Niu, Y. Zhao, S. L. Ho, and W. N. Fu, "A Parameterized Mesh Technique for Finite Element Magnetic Field Computation and Its Application to Optimal Designs of Electromagnetic Devices," *IEEE Trans. Magn.*, vol. 47, no. 10, pp. 2943–2946, Oct. 2011.

[4] S. Niu, N. Chen, S. L. Ho, and W. N. Fu, "Design Optimization of Magnetic Gears Using Mesh Adjustable Finite-Element Algorithm for Improved Torque," *IEEE Trans. Magn.*, vol. 48, no. 11, pp. 4156–4159, Nov. 2012.

[5] Y. Zhao, S. L. Ho, and W. N. Fu, "A Novel Fast Remesh-Free Mesh Deformation Method and Its Application to Optimal Design of Electromagnetic Devices," *IEEE Trans. Magn.*, vol. 50, no. 11, pp. 1–4, Nov. 2014.

[6] L. Yang, S. L. Ho, W. N. Fu, and L. Liu, "A Mesh Deformation Algorithm and Its Application in Optimal Motor Design," *IEEE Trans. Magn.*, vol. 52, no. 3, pp. 1–4, Mar. 2016.

[7] Y. Zhao, X. Xiao, and W. Xu, "Accelerating the Optimal Shape Design of Linear Machines by Transient Simulation Using Mesh Deformation and Mesh Connection Techniques," *IEEE Trans. Ind. Electron.*, vol. 65, no. 12, pp. 9825–9833, Dec. 2018.

[8] D. Kraft, *A software package for sequential quadratic programming*, ser. Forschungsbericht. Deutsche Forschungs- und Versuchsanstalt fr Luft- und Raumfahrt, DFVLR ; 88-28, Kln, 1988.

[9] E. Carraro, M. Morandin, and N. Bianchi, "Traction PMASR Motor Optimization According to a Given Driving Cycle," *IEEE Trans. Ind Appl.*, vol. 52, no. 1, pp. 209–216, Jan. 2016.

[10] A. Fatemi, N. A. O. Demerdash, T. W. Nehl, and D. M. Ionel, "Large-Scale Design Optimization of PM Machines Over a Target Operating Cycle," *IEEE Trans. Ind Appl.*, vol. 52, no. 5, pp. 3772–3782, Sep. 2016.

Stiaan Gerber (M'13) received the Ph.D. degree in electrical engineering from Stellenbosch University, Stellenbosch, South Africa, in 2015. He is currently a Postdoctoral Researcher with the same university. He is an avid software developer and has published more than 20 papers in recognized international journals and conference proceedings. His research interests in the engineering field include electrical machine design, magnetic gear technology, numerical optimization, finite-element methods, and renewable power generation.

Rong-Jie Wang (M'00–SM'08) received the M.Sc. degree in electrical engineering from the University of Cape Town, Cape Town, South Africa, in 1998, and the Ph.D. degree in electrical engineering from Stellenbosch University, Stellenbosch, South Africa, in 2003. He is currently an Associate Professor with the Department of Electrical and Electronic Engineering, Stellenbosch University. In recent years, his work has been focused on the magnetic gear and magnetically geared electrical machine technologies. His research interests include novel topologies of permanent magnet machines, computer-aided design and optimization of electrical machines, cooling design and analysis, and renewable energy systems.